View metadata, citation and similar papers at core.ac.uk

brought to you by CORE

東北大学機関リポジトリ
TOUR
Tohoku University Repository

Plasma mechanisms of resonant terahertz detection in two-dimensional electron channel with split gates

著者	尾辻　泰一
journal or publication title	Journal of Applied Physics
volume	103
number	1
page range	014504-1-014504-6
year	2008
URL	http://hdl.handle.net/10097/47798

doi: 10.1063/1.2828173

Plasma mechanisms of resonant terahertz detection in a two-dimensional electron channel with split gates

V. Ryzhii[a)] and A. Satou
Computer Solid State Physics Laboratory, University of Aizu, Aizu-Wakamatsu 965-8580, Japan

T. Otsuji
Research Institute of Electrical Communication, Tohoku University, Sendai 980-8577, Japan

M. S. Shur
Department of Electrical, Computer, and Systems Engineering, Rensselaer Polytechnic Institute, Troy, New York 12180, USA

(Received 10 September 2007; accepted 2 November 2007; published online 4 January 2008)

We analyze the operation of a resonant detector of terahertz (THz) radiation based on a two-dimensional electron gas (2DEG) channel with split gates. The side gates are used for the excitation of plasma oscillations by incoming THz radiation and control of the resonant plasma frequencies. The central gate provides the potential barrier separating the source and drain portions of the 2DEG channel. Two possible mechanisms of the detection are considered: (1) modulation of the ac potential drop across the barrier and (2) heating of the 2DEG due to the resonant plasma-assisted absorption of THz radiation followed by an increase in thermionic dc current through the barrier. Using the device model, we calculate the frequency and temperature dependences of the detector responsivity associated with both dynamic and heating (bolometric) mechanisms. It is shown that the dynamic mechanism dominates at elevated temperatures, whereas the heating mechanism provides larger contribution at low temperatures, $T \lesssim 35-40$ K.
© *2008 American Institute of Physics*. [DOI: 10.1063/1.2828173]

I. INTRODUCTION

Plasma oscillations in heterostructures with a two-dimensional electron gas (2DEG) and some devices using the excitation of these oscillations have been experimentally studied for decades (see, for instance, Refs. 1–17). There are also many theoretical papers on different aspects of these plasma waves and their potential applications. The gated and ungated 2DEG channels in heterostructures can serve as resonant cavities for terahertz (THz) electron plasma waves.[18] The resonant properties of such channels can be utilized in different THz devices, in particular, resonant detectors.[3–5,9,10,12–17] The mechanism of the THz detection observed in transistor structures[3,4,6,7,9,10,15–17] might be attributed to the nonlinearity of the plasma oscillations as suggested previously.[18] The variation of the conductivity of 2DEG with a periodic gate system can possibly be explained by the heating of 2DEG by absorbed THz radiation (heating or bolometric mechanism).[5,13] Recently, a concept of resonant detectors in which a plasma resonant cavity is integrated with a Schottky junction was proposed and substantiated.[19,20] As shown, when the frequency of incoming THz radiation is close to one of the plasma resonant frequencies, the ac potential drop across the barrier at the Schottky junction becomes resonantly large. This leads to rather large values of the rectified component of the current through the junction, which is used as an output signal of the detector. Since the resonant excitation of the plasma oscillations by absorbed THz radiation leads to the heating of 2DEG, the heating (bolometric) mechanism can also contribute to the rectified current over the Schottky barrier. Thus, two mechanisms can be responsible for the operation of this detector: the dynamic mechanism considered previously[19] and the heating mechanism. Similar mechanisms can work in the detectors utilizing the excitation of plasma oscillations but having the barrier of another origin. In particular, the barrier formed by an additional gate that results in an essential depletion under it was used in recent experiments.[14] In this article, we develop a device model for a THz resonant detector based on a heterostructure with the 2DEG channel and the barrier region utilizing the plasma oscillations excitation. We consider a device with three gates (see Fig. 1): the 2DEG under two extreme gates forms the plasma resonant cavities, while the central gate, to which a sufficiently large negative bias volt-

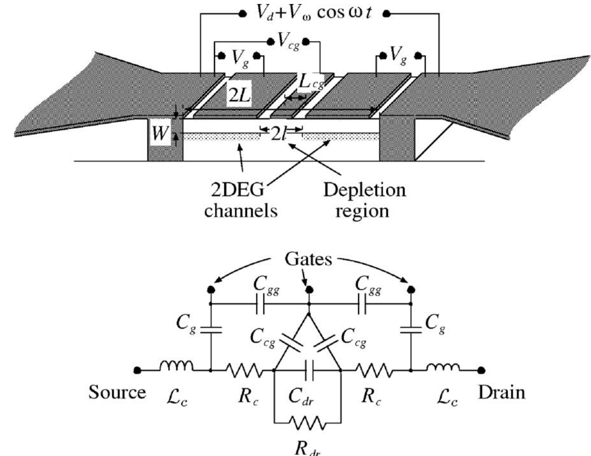

FIG. 1. Schematic view of the THz detector under consideration and its simplified equivalent circuit.

[a)]Electronic mail: v-ryzhii@u-aizu.ac.jp.

 © 2008 American Institute of Physics

Downloaded 14 Mar 2010 to 130.34.135.83. Redistribution subject to AIP license or copyright; see http://jap.aip.org/jap/copyright.jsp

age is applied, forms the barrier. The excitation of the plasma oscillations by the incident THz radiation is assumed to be associated with an antenna connected with the source and drain contacts to the 2DEG channel. In the following, we demonstrate that each of the mechanisms in question can dominate in different temperature ranges (the dynamic mechanism is predominant at elevated temperatures, whereas the heating mechanism provides a larger contribution at low temperatures, $T \lesssim 35-40$ K). The device structure under consideration differs from that studied in Ref. 14, in which the THz radiation input was realized by a periodic grating. However, the physical mechanisms of detection are the same.

II. EQUATIONS OF THE MODEL

We assume that the net drain-source voltage V includes both the dc bias voltage V_d and the ac component $V_\omega \cos \omega t$ induced by incoming THz radiation via an antenna connected with the source and drain contacts. Thus, $V = V_d + V_\omega \cos \omega t$, where ω is the THz radiation frequency. The bias voltage V_g is applied between the side gates and the pertinent contacts. This voltage affects the electron density in the quasineutral portions of the 2DEG channel, so that the dc electron density is given by

$$\Sigma_0 = \Sigma_d + \frac{æ V_g}{4\pi e W}, \tag{1}$$

where e is the electron charge, W is the gate layer thickness, and $æ$ is the dielectric constant. It is also taken to be that the potential drop, V_{cg}, between the central gate and the source contact is negative and its absolute value is sufficiently large to deplete some portion of the 2DEG channel underneath this gate and create a potential barrier. This implies that $V_{cg} < -4\pi e W / æ \Sigma_d = V_{th}$, where V_{th} is the 2DEG threshold voltage.

The ac component of the electric potential in the channel $\delta\varphi$ satisfies the boundary conditions that follow from the fact that at the source and drain contacts, its values coincide with the ac components of the incoming signal voltage,

$$-\delta\varphi|_{x=-L} = \delta\varphi|_{x=+L} = \frac{1}{2} V_\omega \cos \omega t. \tag{2}$$

Assuming that the conductivity of the quasineutral sections is much larger than that of the depletion region (including the thermionic current over the barrier and the displacement current associated with the capacitances shown in the equivalent circuit of Fig. 1), one may use the following additional conditions:

$$\left.\frac{\partial}{\partial x}\delta\varphi\right|_{x=\pm l} \simeq 0. \tag{3}$$

Here $2L$ is the length of the 2DEG channel between the source and drain contacts, $2l > L_{cg}$ is the length of the depletion region under the central gate, and L_{cg} is the length of the latter (see Fig. 1). The quantity l is determined by the potential of the central gate V_{cg}. Definitely, the conductivity of the quasineutral sections markedly exceeds the real part of the depleted region admittance. The role of the displacement current across the depleted region is discussed in Sec. VIII.

The electron transport in the channel is governed by the hydrodynamic equations coupled with the Poisson equation for the self-consistent electric potential.[18] At sufficiently small intensities of THz radiation, this system of equations can be linearized and reduced to the following equation[21,22] valid in the quasineutral regions of the channel ($-L \le x < -l$ and $l < x \le L$):

$$\frac{\partial}{\partial t}\left(\frac{\partial}{\partial t} + \nu\right)\delta\varphi = s^2 \frac{\partial^2}{\partial x^2}\delta\varphi, \tag{4}$$

where ν is the frequency of electron collisions with impurities and phonons, $s = \sqrt{4\pi e^2 \Sigma_0 W / m æ}$ is the plasma wave velocity, and m is the electron effective mass. The effect of electron pressure results in some renormalization of the plasma wave velocity:[23–25] $s\sqrt{(4\pi e^2 \Sigma_0 W / m æ) + s_0^2}$, where s_0 is the velocity of the electron "sound" (usually $s_0 \ll s$).

Assuming that the central gate length is comparable with the gate layer thickness, the shape of the barrier under the central gate can be considered as parabolic: $\Delta_b(x) = \Delta_b[1 - (x/l)^2] - e(V_d + \delta V^b)(l + x)/2l$, where Δ_b is the barrier height in equilibrium (it depends on the potential, V_{cg}, of the central gate), and $V_d + \delta V^b$ is the lateral potential drop across the depletion (barrier) region associated with the dc bias voltage V_d and the ac voltage δV^b. The variation of the barrier height $\delta\Delta_b$ due to the lateral potential drop is given by

$$\delta\Delta_b = -\frac{e(V_d + \delta V^b)}{2}\left(1 - \frac{e(V_d + \delta V^b)}{8\Delta_b}\right) \simeq -\frac{e(V_d + \delta V^b)}{2}. \tag{5}$$

Hence, at $e|V_d + \delta V^b| \ll \Delta_b$, the net source-drain current can be calculated using the following formula:

$$J = J_m \exp\left(-\frac{\Delta_b}{k_B T}\right)\left[\exp\left(\frac{e(V_d + \delta V^b)}{2k_B T}\right) - 1\right], \tag{6}$$

where J_m is the maximum current (for a 2DEG $J_m \propto T^{3/2}$), the ac potential drop, δV^b, across the depletion (barrier) region is given by

$$\delta V^b = \delta\varphi|_{x=+l} - \delta\varphi|_{x=-l} = 2\delta\varphi|_{x=+l}, \tag{7}$$

and $T = T_0 + \delta T$ is the electron temperature, T_0 is the lattice temperature, and δT is the variation of the electron temperature due to THz irradiation.

In this case, at $e\delta V^b < k_B T < \Delta_b$, Eq. (6) yields the following equation for the dc source-drain current J_0:

$$\Delta J_0 = J_0 - J_{00} = J_m \exp\left(-\frac{\Delta_b}{k_B T_0}\right)\exp\left(\frac{eV_d}{2k_B T_0}\right) \times \left(\frac{e^2\overline{(\delta V^b)^2} + 8(\Delta_b - eV_d/2)k_B\overline{\delta T}}{8(k_B T_0)^2}\right) \tag{8}$$

at $eV_d > k_B T_0$ and

Downloaded 14 Mar 2010 to 130.34.135.83. Redistribution subject to AIP license or copyright; see http://jap.aip.org/jap/copyright.jsp

$$\Delta J_0 = J_0 - J_{00} = J_m \exp\left(-\frac{\Delta_b}{k_B T_0}\right)\left(\frac{eV_d}{2k_B T_0}\right) \times \left(\frac{e^2\overline{(\delta V^b)^2} + 8(\Delta_b - eV_d/2)k_B\overline{\delta T}}{8(k_B T_0)^2}\right) \quad (9)$$

at $eV_d \ll k_B T_0$. Here,

$$J_{00} = J_m \exp\left(-\frac{\Delta_b}{k_B T_0}\right)\left[\exp\left(\frac{eV_d}{2k_B T_0}\right) - 1\right] \quad (10)$$

is the dc source-drain current without THz irradiation (dark current).

III. PLASMA RESONANCES

Solving Eq. (4) with boundary conditions (2) and (3) and taking into account Eq. (7), we obtain

$$\delta V^b = \frac{V_\omega}{2}\left(\frac{e^{i\omega t}}{\cos[q_\omega(L-l)]} + \frac{e^{-i\omega t}}{\cos[q_{-\omega}(L-l)]}\right). \quad (11)$$

Here

$$q_{\pm\omega} = \sqrt{\frac{m æ\omega(\omega \mp i\nu)}{4\pi e^2 \Sigma_0 W}}. \quad (12)$$

Equation (11) yields

$$\overline{(\delta V^b)^2} = \frac{V_\omega^2}{2}\left[\cos^2\left(\frac{\pi\omega}{2\Omega}\right) + \sinh^2\left(\frac{\pi\nu}{4\Omega}\right)\right]^{-1}, \quad (13)$$

where

$$\Omega = \sqrt{\frac{\pi^3 e^2 \Sigma_0 W}{æ m (L-l)^2}} \quad (14)$$

is the characteristic plasma frequency. Due to the dependence [given by Eq. (1)] of the dc electron density on the gate voltage V_g, the characteristic plasma frequency Ω can be tuned by this voltage. Because of the dependence of Ω on the length, $L-l$, of the quasineutral sections of the gated 2DEG channel (serving as the resonant plasma cavities) and, hence, on the potential of the central gate V_{cg}, Ω is somewhat varied with varying V_{cg}.

IV. RESONANT ELECTRON HEATING

The power absorbed by the channel can be calculated using the following equation:

$$\delta P_\omega = \frac{2e^2\Sigma_0\nu}{m(\omega^2+\nu^2)}\int_l^L dx \left|\frac{\partial \delta\varphi}{\partial x}\right|^2. \quad (15)$$

Considering Eq. (15), the energy balance equation governing the averaged electron temperature can be presented as

$$\frac{k_B\overline{\delta T}}{\tau_\varepsilon} = \frac{e^2\nu}{m(\nu^2+\omega^2)}\overline{\left(\frac{\delta V^b}{L-l}\right)^2}K, \quad (16)$$

where τ_ε is the electron energy relaxation time. The factor K is associated with the nonuniformity of the ac electric field under the side gates. This factor is given by

$$K = \left(\frac{\pi}{8}\right)^2 \frac{\omega\sqrt{\omega^2+\nu^2}}{\Omega^2}\left[\left(\frac{2\Omega}{\pi\nu}\right)\sinh\left(\frac{\pi\nu}{2\Omega}\right) - \left(\frac{\Omega}{\pi\omega}\right)\sin\left(\frac{\pi\omega}{\Omega}\right)\right]. \quad (17)$$

At $\nu \ll \omega, \Omega$, Eq. (17) yields

$$K = \left(\frac{\pi}{8}\right)^2\left(\frac{\omega}{\Omega}\right)^2\left[1 - \left(\frac{\Omega}{\pi\omega}\right)\sin\left(\frac{\pi\omega}{\Omega}\right)\right], \quad (18)$$

so that one can use the following simplified formula:

$$k_B\overline{\delta T} \simeq \left(\frac{\pi}{8}\right)^2 \frac{e^2\nu\tau_\varepsilon}{mL^2\Omega^2}\overline{(\delta V^b)^2}. \quad (19)$$

V. RECTIFIED CURRENT AND DETECTOR RESPONSIVITY

Using Eqs. (8) and (16), we obtain

$$\Delta J_0 = J_m \exp\left(\frac{V_d - 2\Delta_b}{2k_B T_0}\right)\frac{(1+H)e^2\overline{(\delta V^b)^2}}{8(k_B T_0)^2}, \quad (20)$$

where the term

$$H = \frac{4(2\Delta_b - eV_d)\nu\tau_\varepsilon}{m(\nu^2+\omega^2)(L-l)^2}K \quad (21)$$

is associated with the contribution of the electron heating to the rectified current.

Combining Eqs. (13) and (20), we arrive at

$$\Delta J_0 = J_m \cdot \frac{\exp\left(\frac{V_d - 2\Delta_b}{2k_B T_0}\right)(1+H)}{4\left[\cos^2\left(\frac{\pi\omega}{2\Omega}\right) + \sinh^2\left(\frac{\pi\nu}{4\Omega}\right)\right]}\left(\frac{eV_\omega}{2k_B T_0}\right)^2. \quad (22)$$

Since V_ω^2 is proportional to the incoming THz power, the detector responsivity as a function of the signal frequency and the structural parameters (except the antenna parameters) can be in the following form:

$$R \propto \frac{\exp\left(\frac{V_d - 2\Delta_b}{2k_B T_0}\right)}{\left[\cos^2\left(\frac{\pi\omega}{2\Omega}\right) + \sinh^2\left(\frac{\pi\nu}{4\Omega}\right)\right]}\frac{(1+H)}{\sqrt{k_B T_0}}. \quad (23)$$

As follows from Eq. (23), the responsivity as a function of the frequency of incoming THz radiation exhibits sharp peaks at the plasma resonant frequencies $\omega = \Omega(2n-1)$, where $n = 1, 2, 3, \ldots$ is the resonance index, provided that the quality factor of resonances $\Omega/\nu \gg 1$.

VI. COMPARISON OF DYNAMIC AND HEATING MECHANISMS

As seen from Eq. (22), the ratio of the heating and dynamic components of the rectified dc source-drain current is given by the quantity H (heating parameter). At $\nu \ll \omega, \Omega$, considering Eqs. (18) and (19), the quantity H can be estimated as

Downloaded 14 Mar 2010 to 130.34.135.83. Redistribution subject to AIP license or copyright; see http://jap.aip.org/jap/copyright.jsp

$$H = \frac{\pi^2}{16}\frac{(2\Delta_b - eV_b)\nu\tau_\varepsilon}{m\Omega^2(L-l)^2} \simeq \frac{\pi^2}{8}\frac{\Delta_b \nu\tau_\varepsilon}{m\Omega^2(L-l)^2}. \tag{24}$$

Considering that $\Omega = \pi s/2(L-l)$, Eq. (24) can be presented in the following form:

$$H \simeq \frac{1}{4}\left(\frac{2\Delta_b - eV_d}{ms^2}\right)\nu\tau_\varepsilon \simeq \left(\frac{\Delta_b}{2ms^2}\right)\nu\tau_\varepsilon. \tag{25}$$

The first factor in Eq. (25) is usually small, while the second one can be large, so that H can markedly exceed unity, particularly at low temperatures. In line with the above assumptions, Eqs. (24) and (25) are valid at moderate drain voltages when $\Delta_b - eV_d/2$ is positive and, moreover, not too small in comparison with Δ_b.

It is natural to assume that in a wide range of temperature (from liquid helium to room temperatures), the electron collision frequency (the inverse momentum relaxation time) is determined by the electron interaction with acoustic phonons and charged impurities, while the electron energy relaxation is due to the interaction with both acoustic and polar optical phonons. Hence, $\nu = \nu^{(\mathrm{ac})} + \nu^{(i)}$ and $\tau_\varepsilon = \tau_\varepsilon^{(\mathrm{ac})}\tau_\varepsilon^{(\mathrm{op})}/(\tau_\varepsilon^{(\mathrm{ac})} + \tau_\varepsilon^{(\mathrm{op})})$, where $\nu^{(\mathrm{ac})}$ and $\nu^{(i)}$ are related to the electron scattering on acoustic phonons and impurities (charged), respectively, whereas $\tau_\varepsilon^{(\mathrm{ac})}$ and $\tau_\varepsilon^{(\mathrm{op})}$ are the electron energy relaxation times associated with the acoustic and optical phonons. As a result, the product $\nu\tau_\varepsilon$ can be presented as

$$\nu\tau_\varepsilon = \frac{(\nu^{(\mathrm{ac})} + \nu^{(i)})\tau_\varepsilon^{(\mathrm{ac})}\tau_\varepsilon^{(\mathrm{op})}}{(\tau_\varepsilon^{(\mathrm{ac})} + \tau_\varepsilon^{(\mathrm{op})})}. \tag{26}$$

We shall use the following formulas for the temperature dependences of the parameters in this equation:

$$\nu^{(\mathrm{ac})} = \frac{1}{\bar{\tau}_{\mathrm{PA}}^{(\mathrm{ac})}}\left(\frac{k_BT_0}{\hbar\omega_0}\right)^{1/2} + \frac{1}{\bar{\tau}_{\mathrm{DA}}^{(\mathrm{ac})}}\left(\frac{k_BT_0}{\hbar\omega_0}\right)^{3/2}, \tag{27}$$

$$\frac{1}{\tau_\varepsilon^{(\mathrm{ac})}} = \frac{2ms_a^2}{\hbar\omega_0}\left[\frac{1}{\bar{\tau}_{\mathrm{PA}}^{(\mathrm{ac})}}\left(\frac{k_BT_0}{\hbar\omega_0}\right)^{-1/2} + \frac{1}{\bar{\tau}_{\mathrm{DA}}^{(\mathrm{ac})}}\left(\frac{k_BT_0}{\hbar\omega_0}\right)^{1/2}\right], \tag{28}$$

$$\frac{1}{\tau_\varepsilon^{(\mathrm{op})}} = \frac{1}{\bar{\tau}^{(\mathrm{op})}}\frac{2}{3}\left(\frac{\hbar\omega_0}{k_BT_0}\right)^2\exp\left(-\frac{\hbar\omega_0}{k_BT_0}\right), \tag{29}$$

where $\bar{\tau}_{\mathrm{PA}}^{(\mathrm{ac})} = 8$ ps, $\bar{\tau}_{\mathrm{DA}}^{(\mathrm{ac})} = 4$ ps, and $\bar{\tau}^{(\mathrm{op})} = 0.14$ ps (Ref. 26) are the characteristic scattering times for the acoustic phonon scattering (polar and deformation mechanisms, respectively) and for the optical phonon scattering, and $\hbar\omega_0$ is the optical phonon energy. The temperature dependence of the collision frequency of 2D electrons with charged impurities is assumed to be as follows:

$$\nu^{(i)} = \bar{\nu}^{(i)}\left(\frac{\hbar\omega_0}{k_BT_0}\right)S(|z_i|, k_BT_0/\hbar\omega_0). \tag{30}$$

Here the function[27]

$$S(z_i,\xi) = \int_0^1 \exp(-\alpha|z_i|\sqrt{\xi}x)\frac{dx}{\sqrt{1-x^2}}$$

characterizes a decrease in the collision frequency with increasing thickness of the spacer, $|z_i|$, between the 2DEG

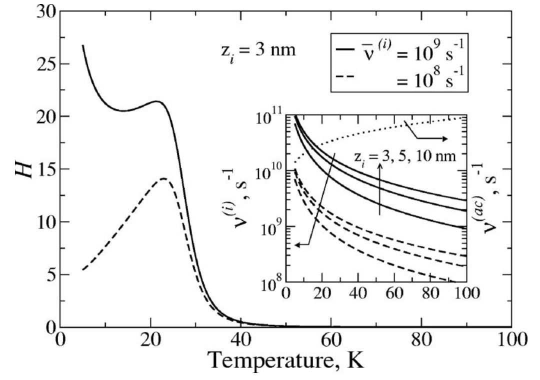

FIG. 2. Temperature dependences of heating parameter H. The inset shows the temperature dependences of the electron collision frequencies associated with impurity and acoustic scattering mechanisms.

channel and the charged donor sheet, and $\alpha = 4\sqrt{2m\hbar\omega_0}/\hbar \simeq 10^7$ cm^{-1}. The characteristic frequency $\bar{\nu}_i$ is proportional to the donor sheet density. We set $\bar{\nu}^{(i)} = (10^8 - 10^9)$ s^{-1}. At $T_0 = 4.2$ K, these values correspond to $\nu^{(i)} = 10^{10} - 10^{11}$ s^{-1} and the electron mobilities $\mu \simeq (10^5 - 10^6)$ cm^2/V s. When $|z_i| = 0$, Eq. (30) yields $\nu_i \propto T_0^{-1}$, while at sufficiently thick spacers, one obtains $\nu_i \propto T_0^{-3/2}$. In the case of relatively thick electron channels, in which the quantization is insignificant, $\nu_i \propto T_0^{-3/2}$.

Figure 2 shows the temperature dependence of the "heating" parameter H, which determines the relative contribution of the heating mechanism to the detector responsivity, calculated for different values of parameter $\bar{\nu}^{(i)}$, i.e., different doping levels. It is assumed that for a GaAs channel $\hbar\omega_0/k_B = 421$ K.[26] We set $s = 1 \times 10^8$ cm/s, $s_a = 5 \times 10^5$ cm/s, the barrier height $\Delta_b = 110$ meV, and the bias voltage $V_d = 20$ mV, so that the effective barrier height $\Delta_b^{(\mathrm{eff})} = \Delta_b - eV_b/2 = 100$ meV. As seen from Fig. 2, the heating mechanism can provide a significantly larger contribution to the detector responsivity at low temperatures ($T_0 \lesssim 35-40$ K). However at elevated temperatures, this mechanism becomes relatively inefficient. This is attributed to weak electron heating due to strong energy relaxation on optical phonons at elevated temperature.

VII. TEMPERATURE DEPENDENCES OF THE DETECTOR RESPONSIVITY AND DETECTIVITY

As mentioned in Sec. V, the detector responsivity exhibits its sharp peaks at the plasma resonant frequencies $\omega = \Omega(2n-1)$. The sharpness of these peaks depends on the electron collision frequency ν, which in turn depends on the temperature.

As follow from Eq. (23), the maximum values of the detector responsivity at the fundamental resonance ($n=1$) are given by

$$\max R \propto \frac{\exp\left(\frac{V_d - 2\Delta_b}{2k_BT_0}\right)}{\sinh^2\left(\frac{\pi\nu}{4\Omega}\right)}\frac{(1+H)}{\sqrt{k_BT_0}}. \tag{31}$$

As a result, for the value of the ratio of the detector responsivity at the resonance and the dark current, one obtains

Downloaded 14 Mar 2010 to 130.34.135.83. Redistribution subject to AIP license or copyright; see http://jap.aip.org/jap/copyright.jsp

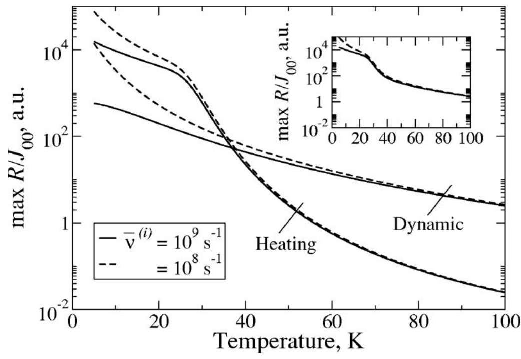

FIG. 3. Temperature dependences of dynamic and heating contributions to max R/J_{00}, of the detector responsivity maximum (resonant) value and the dark current. The inset shows the net value max R/J_{00} as a function of temperature.

$$\frac{\max R}{J_{00}} \propto \frac{1}{\sinh^2\left(\frac{\pi\nu}{4\Omega}\right)} \frac{1+H}{(k_B T)^2}. \tag{32}$$

Figure 3 shows the temperature dependences of the maximum (resonant) values of the dynamic and heating contributions to the detector responsivity divided by the dark current value calculated using Eq. (32) for the barrier height $\Delta_b^{(\mathrm{eff})}=100$ meV, the fundamental plasma frequencies $\Omega/2\pi=1$ THz, and different values of the parameter $\bar{\nu}^{(i)}$. The inset shows the temperature dependence of max R/J_{00}, which accounts for both mechanisms.

Taking into account that the detector detectivity $D^* \propto R/\sqrt{J_{00}}$, we arrive at the following formula:

$$\max D^* \propto \frac{\exp\left(\frac{V_d - 2\Delta_b}{4k_B T_0}\right)}{\left[\sinh^2\left(\frac{\pi\nu}{4\Omega}\right)\right]} \frac{(1+H)}{(k_B T_0)^{5/4}}. \tag{33}$$

Figure 4 shows the temperature dependences of the detector detectivity calculated for different values of the effective barrier height $\Delta_b^{(\mathrm{eff})}=\Delta_b - eV_d/2$.

As follows from the above formulas, the detector responsivity and detectivity increase with decreasing effective barrier height. However, this quantity cannot be set too small (at a given temperature T_0) in the frame of our model, which is valid if $\Delta_b^{(\mathrm{eff})} \gg k_B T_0$, and when the 2DEG channel can be partitioned into the quasineutral and deleted sections.

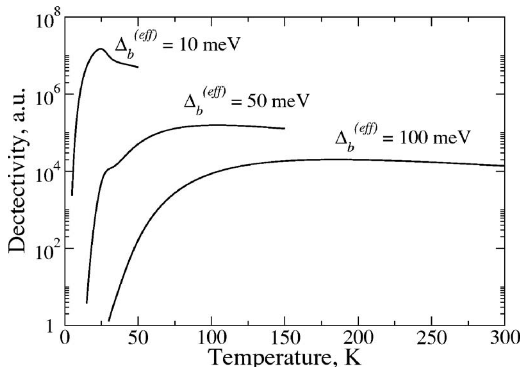

FIG. 4. Temperature dependences of the detector detectivity D^* for different values of the effective barrier height $\Delta_b^{(\mathrm{eff})}$.

VIII. DISCUSSION

The displacement current across the depleted region can be, in principle, essential. To take this current into consideration, one needs to modify Eq. (3).[28] Introducing the admittance, Y_ω, of the barrier region, we can use the following boundary conditions at the edge of the quasineutral sections of the 2DEG channel (for the asymmetrical plasma modes for which $\delta\varphi_\omega|_{x=-l} = -\delta\varphi_\omega|_{x=l}$):

$$-\sigma_\omega \frac{d\varphi_\omega}{dx}\bigg|_{x=\pm l} = 2Y_\omega \delta\varphi_\omega|_{x=\pm l}. \tag{34}$$

Here, $\sigma_\omega = -i[e^2\Sigma_0/m(\omega+i\nu)]$ is the ac conductivity of the quasineutral sections of the channel accounting for the electron collisions and inertia. Since the real part of the conductivity of the depleted (barrier) region is definitely small in comparison with the conductivity of the quasineutral sections, one can take into account only the capacitive component of the current across the depleted region. In this case, $Y_\omega = -i\omega C$, where C is the pertinent capacitance, which is determined by the capacitances C_{cg} and C_{dr}: $C = C_{\mathrm{dr}} + C_{\mathrm{gs}}/2$ (see the equivalent circuit in Fig. 1). This equivalent circuit accounts for the inductance of the quasineutral sections $\mathcal{L}_c$, due to the inertia of the electron transport along the channel, the channel resistance due to the electron scattering, the resistance of the barrier region R_{dr}, and different capacitances. Equation (34) can be presented in the form

$$\frac{\Omega^2(L-l)}{\omega(\omega+i\nu)} \frac{d\delta\varphi_\omega}{dx}\bigg|_{x=\pm l} = c\,\delta\varphi_\omega|_{x=\pm l}, \tag{35}$$

where

$$c = \frac{2\pi^2 CW}{\text{æ}(L-l)} \simeq \frac{2\pi^2 CW}{\text{æ}L}. \tag{36}$$

If the parameter $c \ll 1$, Eqs. (3) and (35) practically coincide (except the case $\omega \gg \Omega$). According to Ref. 28, $C_{\mathrm{dr}} = (\text{æ}/2\pi^2)\Lambda_{\mathrm{dr}}$ and $C_{\mathrm{cg}} = (\text{æ}/2\pi^2)\Lambda_{\mathrm{cg}}$, where Λ_{dr} and Λ_{dr} are logarithmic factors that are determined by the geometry of the planar conducting areas (the gates and quasineutral sections of the channel). These factors can be estimated as[28] $\Lambda_{\mathrm{dr}} \sim \Lambda_{\mathrm{cg}} \sim \ln(2L/l)$. Hence, $c \simeq (W/L)\Lambda$, where $\Lambda = \Lambda_{\mathrm{dr}} + \Lambda_{\mathrm{cg}}/2$. The factor Λ somewhat exceeds unity, although it is not too large. Thus, taking into account that $W \ll L$, one can conclude that for real device structures, $c \ll 1$. The condition of the smallness of c can also be presented in the form $C_g \gg C$, where $C_g = \text{æ}4\pi W \simeq L/W$ is the capacitance of the side gates (see Fig. 1). Relatively small capacitances C_{dr} and C_{cg} can, to some extent, affect the plasma oscillations. However, their role reduces mainly to a small modification in the resonant plasma frequencies.[28]

If c would be large, the ac potential near the edges of the quasineutral regions is small as well as the ac potential drop across the depleted region. This implies that the boundary condition (34) could be $\delta\varphi_{\omega|_{x=\pm l}} \simeq 0$. In such a case, the fundamental plasma frequency is doubled and the dynamic mechanism is weakened. However, the details of the ac potential distribution near the edges of the quasineutral regions are not crucial for the heating mechanism.

Downloaded 14 Mar 2010 to 130.34.135.83. Redistribution subject to AIP license or copyright; see http://jap.aip.org/jap/copyright.jsp

Actually, there is some delay in the electron transit across the barrier. The delay time can be estimated as $\tau_b \simeq 2l/v_T$, where $v_T \simeq \sqrt{k_B T_0/m}$ is the thermal electron velocity. The delay in the electron transit and, therefore, the electron transit time effects can be disregarded if $\omega\tau_b \sim \Omega\tau_b < 1$.[29] Assuming $\Omega/2\pi = 1$ THz and $v_T = 10^7$ cm/s, from the last inequality we obtain $2l < 0.6$ μm.

IX. CONCLUSIONS

We developed a device model for a resonant detector of THz radiation based on the gated 2DEG channel with an electrically induced barrier. The model accounts for the resonant excitation of the plasma oscillations in the gated 2DEG channel as well as the rectified dc current through the barrier. As shown, this current comprises two components: the dynamic component associated with the ac potential drop across the barrier and the heating (bolometric) component due to a change in the electron temperature, which stems from the resonant plasma-assisted absorption of THz radiation. Using our model, we calculated the frequency and temperature dependences of the detector responsivity. The detector responsivity exhibits sharp resonant peaks at the frequencies of incoming THz radiation corresponding to the plasma resonances in the gated 2DEG channel. The plasma resonances can be tuned by the gate voltage V_{cg} and, to some extent, by the potential of the central gate V_{cg}. It is demonstrated that the dynamic mechanism dominates at elevated temperatures, whereas at low lattice temperatures ($T_0 \lesssim 35-40$ K for AlGaAs/GaAs-based detectors), the heating mechanism prevails. This can be attributed to a marked increase in the electron energy relaxation time τ_ε with decreasing lattice temperature.

At rather low temperatures when the ratio $\Delta_b^{(\mathrm{eff})}/k_B T_0$ is large, the thermionic electron current over the barrier can be surpassed by the tunneling current. The rectified portion of this current can be associated with both dynamic and heating mechanisms (the thermo-assisted tunneling current in the case of the latter mechanism). This, however, requires a separate detailed study.

In the case of detection of THz radiation modulated at some frequency $\omega_m \ll \omega$, the relative contributions of the dynamic and heating mechanisms to the responsivity, R^m, characterizing the detector response at the frequency ω_m can be different from those considered above. This is due to different inertia of these mechanisms. In particular, if $\omega_m > \tau_\varepsilon^{-1}$ (but $\omega_m \ll \omega$), the variation of the electron effective temperature averaged over the THz oscillations $\overline{\delta T_m} \simeq \overline{\delta T}/\omega_m\tau_\varepsilon$, i.e., $\overline{\delta T_m} \ll \overline{\delta T}$. As a result, $R_m/R \simeq (\omega_m\tau_\varepsilon)^{-1}$. This implies that even at low temperatures, the heating mechanism can be inefficient if $\omega_m > \tau_\varepsilon^{-1}$.

Both dynamic and heating mechanisms might be responsible for the THz detection in the plasmonic resonant detectors utilizing another barrier structure (for instance, with the lateral Schottky barrier[19,20] or with electron transport through the gate barrier[30–32]) and other types of the plasma resonant cavity (with ungated quasineutral regions as in high-electron mobility transistors with relatively long ungated source-gate and gate-drain regions), as well as in those with other methods of excitation of plasma oscillations (utilizing periodic gate structures[14]).

ACKNOWLEDGMENTS

This work was supported by a Grant-in-Aid for Scientific Research (S) from the Japan Society for the Promotion of Science, Japan. The work at RPI was partially supported by the Office of Naval Research.

[1] S. J. Allen, Jr., D. C. Tsui, and R. A. Logan, Phys. Rev. Lett. **38**, 980 (1977).
[2] D. C. Tsui, E. Gornik, and R. A. Logan, Solid State Commun. **35**, 875 (1980).
[3] W. Knap, Y. Deng, S. Rumyantsev, J.-Q. Lu, M. S. Shur, C. A. Saylor, and L. C. Brunel, Appl. Phys. Lett. **80**, 3433 (2002).
[4] W. Knap, Y. Deng, S. Rumyantsev, and M. S. Shur, Appl. Phys. Lett. **81**, 4637 (2002).
[5] X. G. Peralta, S. J. Allen, M. C. Wanke, N. E. Harff, J. A. Simmons, M. P. Lilly, J. L. Reno, P. J. Burke, and J. P. Eisenstein, Appl. Phys. Lett. **81**, 1627 (2002).
[6] W. Knap, J. Lusakowski, T. Parently, S. Bollaert, A. Cappy, V. V. Popov, and M. S. Shur, Appl. Phys. Lett. **84**, 2331 (2004).
[7] J. Lusakowski, W. Knap, N. Dyakonova, L. Varani, J. Mateos, T. Gonzales, Y. Roelens, S. Bullaert, A. Cappy, and K. Karpierz, J. Appl. Phys. **97**, 064307 (2005).
[8] T. Otsuji, M. Hanabe, and O. Ogawara, Appl. Phys. Lett. **85**, 2119 (2004).
[9] F. Teppe, D. Veksler, V. Yu. Kacharovskii, A. P. Dmitriev, X. Xie, X.-C. Zhang, S. Rumyantsev, W. Knap, and M. S. Shur, Appl. Phys. Lett. **87**, 022102 (2005).
[10] F. Teppe, W. Knap, D. Veksler, M. S. Shur, A. P. Dmitriev, V. Yu. Kacharovskii, and S. Rumyantsev, Appl. Phys. Lett. **87**, 052107 (2005).
[11] M. Hanabe, T. Otsuji, T. Ishibashi, T. Uno, and V. Ryzhii, Jpn. J. Appl. Phys., Part 1 **44**, 3842 (2005).
[12] M. Lee, M. C. Wanke, and J. L. Reno, Appl. Phys. Lett. **86**, 033501 (2005).
[13] E. A. Shaner, M. Lee, M. C. Wanke, A. D. Grine, J. L. Reno, and S. J. Allen, Appl. Phys. Lett. **87**, 193507 (2005).
[14] E. A. Shaner, A. D. Grine, M. C. Wanke, M. Lee, J. L. Reno, and S. J. Allen, IEEE Photonics Technol. Lett. **18**, 1925 (2006).
[15] D. Veksler, F. Teppe, A. P. Dmitriev, V. Yu. Kacharovskii, W. Knap, and M. S. Shur, Phys. Rev. B **73**, 125328 (2006).
[16] A. El Fatimy, F. Teppe, N. Dyakonova, W. Knap, D. Seliuta, G. Valusis, A. Shcherepetov, Y. Roelens, S. Bollaert, A. Cappy, and S. Rumyantsev, Appl. Phys. Lett. **89**, 131926 (2006).
[17] J. Torres, P. Nouvel, A. Akwaoue-Ondo, L. Chusseau, F. Teppe, A. Shcherepetov, and S. Bollaert, Appl. Phys. Lett. **89**, 201101 (2006).
[18] M. Dyakonov and M. Shur, IEEE Trans. Electron Devices **43**, 1640 (1996).
[19] V. Ryzhii and M. S. Shur, Jpn. J. Appl. Phys., Part 2 **45**, L1118 (2006).
[20] A. Satou, N. Vagidov, and V. Ryzhii, IEICE Tech. Rep. ED2006-197, p. 77 (2006).
[21] A. Satou, V. Ryzhii, I. Khmyrova, M. Ryzhii, and M. S. Shur, J. Appl. Phys. **95**, 2084 (2004).
[22] V. Ryzhii, A. Satou, W. Knap, and M. S. Shur, J. Appl. Phys. **99**, 084507 (2006).
[23] S. Rudin and T. L. Reinecke, Phys. Rev. B **54**, 2791 (1996).
[24] F. J. Crowne, J. Appl. Phys. **82**, 1242 (1997).
[25] S. Rudin and G. Samsonidze, Phys. Rev. B **58**, 16369 (1998).
[26] V. F. Gantmakher and Y. B. Levinson, *Carrier Scattering in Metals and Semiconductors* (North-Holland, Amsterdam, 1987).
[27] A. Shik, *Quantum Wells* (World Scientific, Singapore, 1997).
[28] V. Ryzhii, A. Satou, I. Khmyrova, M. Ryzhii, T. Otsuji, V. Mitin, and M. S. Shur, J. Phys.: Conf. Ser. **38**, 228 (2006).
[29] V. Ryzhii and M. S. Shur, Phys. Status Solidi A **202**, R113 (2005).
[30] V. Ryzhii, I. Khmyrova, and M. Shur, J. Appl. Phys. **88**, 2868 (2000).
[31] I. Khmyrova and V. Ryzhii, Jpn. J. Appl. Phys., Part 1 **39**, 4727 (2000).
[32] A. Satou, V. Ryzhii, I. Khmyrova, and M. S. Shur, Semicond. Sci. Technol. **18**, 460 (2003).

Downloaded 14 Mar 2010 to 130.34.135.83. Redistribution subject to AIP license or copyright; see http://jap.aip.org/jap/copyright.jsp